Potential Evaluation on Model Predictive Control-Based Demand Response of a Vapor-Compression Type Air-Conditioning System

Ryuto Mayumi [a], Reona Nishikawa [b], and Tetsuya Wakui [c]

[a] *Department of Mechanical Engineering, Osaka Metropolitan University, Osaka, Japan, sq25759s@st.omu.ac.jp*
[b] *Department of Mechanical Engineering, Osaka Metropolitan University, Osaka, Japan, si24028c@st.omu.ac.jp*
[c] *Department of Mechanical Engineering, Osaka Metropolitan University, Osaka, Japan, t-wakui@omu.ac.jp,* ***CA***

Abstract:

Stabilizing the power demand-supply relationship is necessary to support renewable energy-based power generation. In this study, we develop a model predictive control-based demand response framework for individual vapor-compression type air-conditioning systems (VCSs) to assess their demand response potential. This framework comprises a model predictive controller, a VCS linearizer, and a PMV calculator. In the model predictive controller, we sequentially solve the optimal control problem using a receding horizon approach. The weighted sum to be minimized includes electricity cost, any shortfall in power reduction during demand response, variations in compressor speed, and the margin of the indoor temperature from its upper limit. The indoor comfort constraint considers temperature limits given by the PMV calculator. To address VCS nonlinearity, a linear model is regenerated in response to changes in the VCS operating point and in indoor and ambient temperatures; this model is then given to the model predictive controller. The control horizon length varies based on demand response requests. We apply the framework to assess the demand response potential of a VCS in an office building. Results indicate that fulfilling demand response requests depends on the requested power reduction and VCS pre-cooling, both notably influenced by ambient temperature. Both upper and lower limits of demand response potential are alsoobserved.

Keywords:

Vapor Compression-Type Refrigeration Cycle; Model Predictive Control; Demand Response; Optimization.

1. Introduction

The movement toward decarbonization is accelerating globally. Energy savings are also required in the air conditioning for many sectors. Vapor-compression type air-conditioning systems (VCSs), which are driven by electric power, are widely used in commercial and residential sectors. Generally, the coefficient of performance (COP) of VCSs decreases with the increase in their cooling/heating capacity; this means that the power consumption nonlinearly increases with the cooling/heating capacity. To achieve energy savings in VCS operation, the power consumption should be reduced; however, indoor comfort would be impaired by reducing the low cooling/heating capacity. Thus, the control paradigm of VCSs should be shifted from a conventional control, in which the cooling/heating capacity is passively manipulated in response to variations in the indoor temperature. Active control of VCSs to balance their cooling/heating capacity with variations in the cooling/heating loads is effective from the perspective of energy savings and indoor comfort [1]. Stabilization of electric power supply and demand in power grids is also an important issue to achieve decarbonization with a drastic increase in the installed capacity of renewable energy-based power generation. However, seasonal, daily, and hourly variations in their power outputs significantly affect energy supply-demand balances; thus, a demand response, in which the electric power consumption is actively manipulated on the demand side, should be employed [2]. VCSs are regarded as a demand response resource. For VCS applications, it should also be noted that indoor comfort must be satisfied during their demand-response operation. Interestingly, the energy-saving and demand-response operations of VCSs are common in employing active control considering an indoor comfort constraint. Hence, the development of an active control strategy of VCSs for both energy-saving and demand-response operations contributes to the achievement of decarbonization.

To actively conduct energy-saving operations of VCSs, model predictive control methods have been studied, in which the indoor environment of the air-conditioned rooms is controlled by the manipulation of the cooling

capacity of the VCSs in the upper level and the cooling capacity is further controlled by their operating conditions, e.g., the compressor inlet pressure in the lower level. Dullinger et al. [3] developed a model predictive control, in which the future control strategy of indoor comfort and VCSs is optimized by using the predicted disturbances and the current operation states. However, the computational time to solve the optimal control problems is a critical issue for real-time control. Elliott et al. [4] developed a hierarchical control method consisting of an upper-level model predictive control for the indoor comfort and a high COP operation, and a lower-level feedback control of VCSs with slow responses. Previous studies on model predictive control for demand responses by air-conditioning systems have also been reported. Wang et al. [5] developed a model predictive control framework for the demand response of residential VCSs. In this framework, the electric power cost is just minimized by determining the compressor speed under a given time-of-use electric power price. Tang et al. [6] developed a model predict control for demand response using a chiller-based heating, ventilation, and air-conditioning system, in which the electric power cost is minimized under a time-variant electric power price. The nonlinear performances of the chillers are modeled by using a deep learning technique with physical constraints. Wang et al. [7] constructed a model predictive control-based demand response framework for an inverter-driven VCS, in which the electric power cost is minimized under a real-time electric power pricing structure. The VCS performances were modeled by identifying using its experimental data. In these studies [5–7], the demand response is based on time-variant electric power prices.

The present study developed a model predictive control-based demand response framework for individual VCSs to assess the demand response potential. This framework comprises a model predictive controller, a VCS linearizer, and a PMV calculator. In the model predictive controller, we sequentially solve the optimal control problem using a receding horizon approach. The weighted sum to be minimized includes electricity cost, any shortfall in power reduction during demand response, variations in compressor speed, and the margin of the indoor temperature from its upper limit. The indoor comfort constraint considers temperature limits given by the PMV calculator. To address the nonlinearity of VCS performances, a linear model is regenerated in response to changes in the VCS operating point and in indoor and ambient temperatures; this model is then given to the model predictive controller. Unlike the previous studies on demand responses using time-variant electric power prices [5–7], the demand response request from a capacity market, which is invoked depending on energy supply-demand balances in power grids, is incorporated into the model predictive control framework. Moreover, the indoor comfort can be evaluated by using PMV based on indoor humidity as well as indoor temperature. The developed framework is applied to the potential assessment of the demand response by a VCS in an office building. The requested reduction in the power consumption is parametrically varied on candidate days for activating the demand response.

2. Vapor-Compression Type Air-Conditioning System

The configuration of a VCS in the cooling operation mode is shown in Fig. 1. This VCS consists of an outdoor unit with an inverter-driven compressor and a condenser, and an indoor unit with an expansion valve and an evaporator. Multiple outdoor and indoor units can be involved in the VCS. Indoor units are installed in the air-conditioned rooms; thus, the controlled objects of the present study are the VCS and the air-conditioned rooms. For the VCS, the two operation controls are conducted. The compressor inlet pressure is controlled by manipulating the compressor speed to obtain the required cooling capacity. The degree of superheat of the refrigerant at the evaporator outlet is controlled by manipulating the expansion valve opening to prevent the inflow of wet saturated vapor of the refrigerant to the compressor.

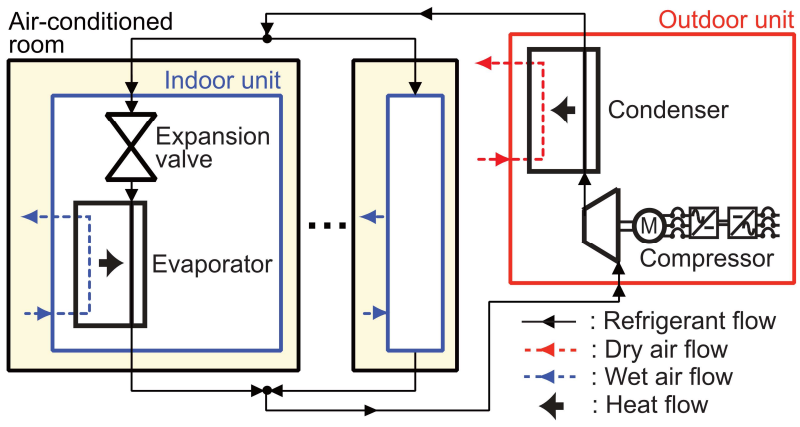

Figure 1: Configuration diagram of vapor-compression type air-conditioning system (VCS) including air-conditioned room

3. Demand response in Japanese Capacity Market

The present study focuses on the demand response incorporated into the Japanese capacity market [8]. The capacity market aims to secure capacity for future power supply, measured by kW instead of kWh, under the large-scale introduction of renewable energy-based power generation. In this market, demand response conducted by aggregators is also regarded as a power supply resource. The scheme of the demand response in the Japanese capacity market is shown in Fig. 2. In this demand response, the reduction in the power consumption from the baseline operation S_{DR} (kW) is previously contracted with a capacity market aggregator. The demand response request is noticed H_{P} (h) before the start of the demand response period, i.e., H_{DR} (h). Due to the contract, the demand response request must be met; however, the maximum number of times of invoking the demand response in one year is established. The achievement of the demand response is evaluated at the time slot of ΔT_{DR} (h); thus, the reduction in the power consumption of the VCS is evaluated I_{DR} times, i.e., $I_{\mathrm{DR}} = H_{\mathrm{DR}}/\Delta T_{\mathrm{DR}}$. A basic incentive to participate in the demand response scheme, a metered incentive for further reduction in power consumption from the contracted S_{DR}, and an unachieved penalty depend on aggregators. In the current Japanese capacity market, the demand response period H_{DR} is three hours; the evaluation interval for the demand response achievement ΔT_{DR} is 30 minutes; the evaluation times of the demand response achievement I_{DR} is six; and the advanced notice period H_{P} is three hours.

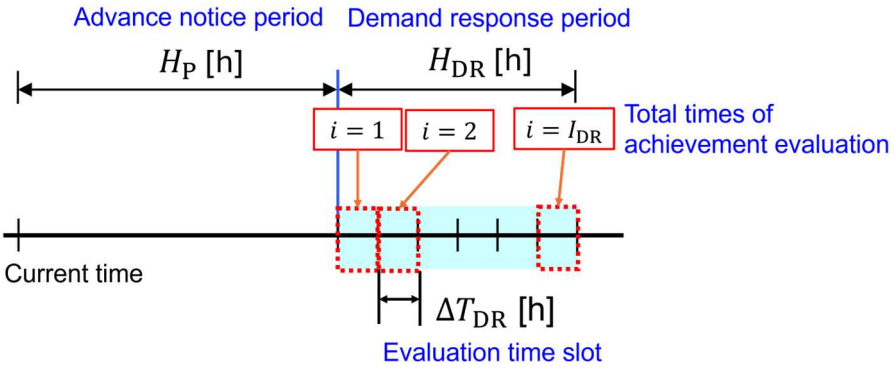

Figure 2: Demand response scheme in Japanese capacity market.

4. Model Predictive Control-Based Demand Response of a Vapor-Compression Type Air-Conditioning System

4.1. Overview

The hierarchical demand response framework, consisting of an upper-level model predictive control of the indoor environment of the air-conditioned rooms and the power consumption to the demand response request and a lower-level multiple feedback controls of the VCS, is shown in Fig. 3. This is an extension of our previous hierarchical control framework [1]. In the upper level, the control planning of the VCS is optimized under the satisfaction of the indoor comfort constraint and the demand response constraint. In the lower level, multiple feedback controls are employed to track the control planning derived in the upper level. By combining the feedforward control based on the derived control planning, the tracking capability is enhanced. The optimal control planning is sequentially performed by using a receding horizon approach; the control planning can be revised in accordance with disturbance variations and prediction errors. The hierarchical demand response framework is also effective from the viewpoint of real-time control because the computation time to solve the optimal control problem is ensured by setting the upper-level control interval to be longer than the lower-level control interval; this can be achieved by the difference in the response speed between the indoor environment and the VCS. The present study on the potential assessment of demand response using VCS focuses on the upper-level model predictive control.

4.2. Model predictive control considering demand response

The details of the optimizer block in Fig. 3 for the upper-level model predictive control are shown in Fig. 4. This optimizer is composed of a model predictive controller, a VCS linearizer, and a PMV calculator. The VCS linearizer and PMV calculator are the preprocessors. In the model predictive controller, the optimal control planning of the VCS in the control horizon is determined by predicting the variations in states of the VCS and

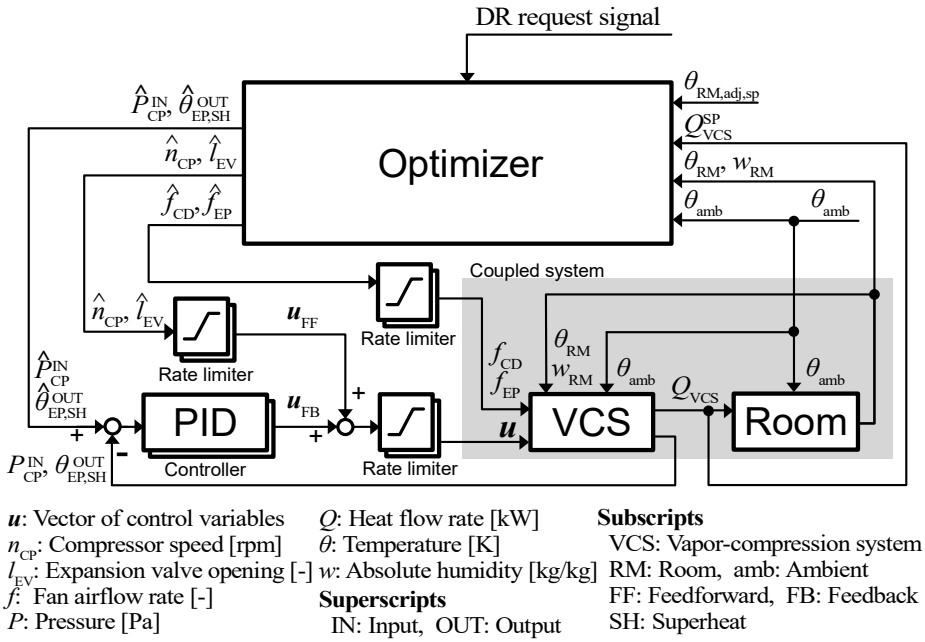

Figure 3: Hierarchical demand response framework using model predictive control and multiple feedback controls.

the air-conditioned room based on the predictor outputs and measured values of the current states of the VCS and the air-conditioned room. The objective of the model predictive control is to maintain the indoor comfort of the air-conditioned rooms, to reduce the power consumption of the VCS, and to achieve the demand response request. The constraint of the power consumption reduction from the baseline operation is added during the demand response period. To enhance the control flexibility of the VCS, the lower and upper limits of the indoor temperature, which are calculated based on PMV evaluation, are utilized as the indoor comfort constraint. Only the control planning result at the first sampling time is applied to the lower-level control. At the next sampling time, the new optimal control planning is carried out by updating the predictor outputs and measured values of the current states of the VCS and air-conditioned room. This is a typical receding horizon approach.

4.2.1. Model predictive controller

The core function of the upper-level control is the optimal control problem in the model predictive controller of Fig. 4. In this controller, the control planning of the VCS in the control horizon $[t_k, t_{k+N_C}]$ is determined so as to minimize the objective function value evaluating the power consumption, the demand response achievement, the compressor speed variations of the VCS, and the margin of the indoor temperature comfort. The control horizon length is dynamically changed in accordance with the demand response request; this means that the value of total sampling times N_C is varied dynamically. The variations in the sensible and latent cooling loads, ambient temperature in the control horizon, and the current indoor temperature and absolute humidity are provided as parameters. In the present study, the cooling load and ambient temperature in the control horizon

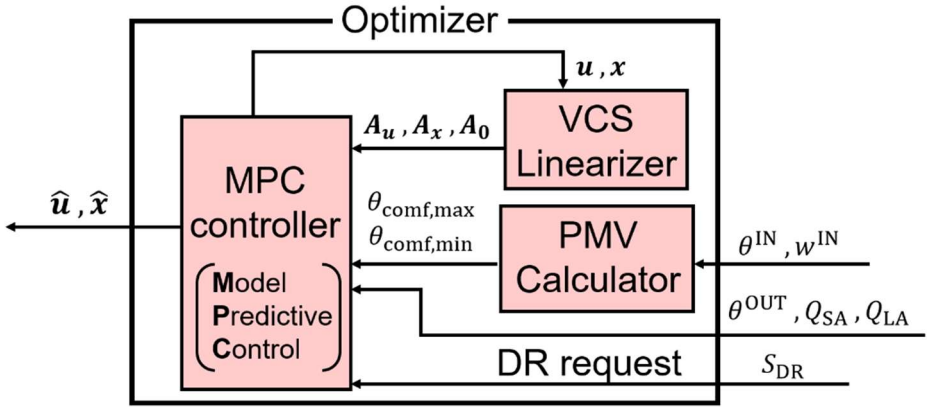

Figure 4: Optimizer in model predictive controller.

are assumed to be predicted perfectly. The achievement of the demand response request, the static performances of the VCS, and the dynamic variations in the indoor temperature and absolute humidity are considered as the constraints. The followings are the details of the optimal control problem.

4.2.1.1. Decision variables

The decision variables of this problem are the VCS output $\boldsymbol{y}_{\mathrm{VCS}}$, the control input $\boldsymbol{u}_{\mathrm{VCS}}$, and the states of the air-conditioned room $\boldsymbol{x}_{\mathrm{RM}}$, as well as the artificial variables expressing the shortfall in the power consumption reduction during the demand response period $\varepsilon_{\mathrm{DR}}^{\mathrm{S}}$.

4.2.1.2. Constraints

The constraints are the static model of the VCS, the dynamic model of the air-conditioned room, the indoor comfort constraint, the operational constraints of the VCS, and the demand response constraints. Equation (1) expresses the static model of the VCS in the control horizon as a time-invariant linear equation [1]:

$$\boldsymbol{y}_{\mathrm{VCS}}(t_j) = \boldsymbol{A}_{\mathrm{U}}(t_k)\boldsymbol{u}_{\mathrm{VCS}}(t_j) + \boldsymbol{A}_{\mathrm{X}}(t_k)\boldsymbol{x}_{\mathrm{RM}}(t_j) + \boldsymbol{A}_0(t_k) \qquad (j = k, k+1, \cdots, k+N_{\mathrm{C}}) \tag{1}$$

where the coefficient matrices $\boldsymbol{A}_{\mathrm{U}}$, $\boldsymbol{A}_{\mathrm{X}}$, and $\boldsymbol{A}_0$ were sequentially calculated in the VCS linearizer before solving the optimal control problem. The dynamic state of the air-conditioned room is modeled as a lumped parameter system. Based on the literature [9], Eq. (2) expressing the dynamic balances of the sensible and latent heats is formulated:

$$\left.\begin{aligned} C_{\mathrm{S}}\frac{\theta_{\mathrm{RM}}(t_{j+1}) - \theta_{\mathrm{RM}}(t_j)}{\Delta T} &= Q_{\mathrm{S}}^{\mathrm{L}}(t_j) - q_{\mathrm{S}}(t_j) \\ C_{\mathrm{L}}\frac{w_{\mathrm{RM}}(t_{j+1}) - w_{\mathrm{RM}}(t_j)}{\Delta T} &= Q_{\mathrm{L}}^{\mathrm{L}}(t_j) - q_{\mathrm{L}}(t_j) \end{aligned}\right\} \qquad (j = k, k+1, \cdots, k+N_{\mathrm{C}}) \tag{2}$$

where θ_{RM} and w_{RM} are the indoor temperature and absolute humidity, respectively; q_{S} and q_{L} are the sensible and latent cooling output of the VCS, respectively; C_{S} and C_{L} are the parameters expressing the heat capacity of the dry air and moisture, respectively; ΔT is the parameter expressing the upper-level control interval; and $Q_{\mathrm{S}}^{\mathrm{L}}$ and $Q_{\mathrm{L}}^{\mathrm{L}}$ are the parameters expressing the sensible and latent cooling loads, respectively, and correspond to the predictor outputs. The indoor temperature and absolute humidity at the sampling time of t_k are given as the measured parameters:

$$\left.\begin{aligned} \theta_{\mathrm{RM}}(t_k) &= \Theta_{\mathrm{RM}}(t_k) \\ w_{\mathrm{RM}}(t_k) &= W_{\mathrm{RM}}(t_k) \end{aligned}\right\} \tag{3}$$

Equation (4) shows the indoor comfort constraint, in which the indoor temperature θ_{RM} can be varied within the range between the lower and upper limits, $\underline{\Theta}_{\mathrm{RM}}$ and $\bar{\Theta}_{\mathrm{RM}}$, respectively.

$$\underline{\Theta}_{\mathrm{RM}}(t_j) \le \theta_{\mathrm{RM}}(t_j) \le \bar{\Theta}_{\mathrm{RM}}(t_j) \qquad (j = k+1, \cdots, k+N_{\mathrm{C}}+1) \tag{4}$$

$\underline{\Theta}_{\mathrm{RM}}$ and $\bar{\Theta}_{\mathrm{RM}}$ are calculated in the PMV calculator. Unlike our previous study [1], no violation of this constraint is considered because the demand response request is preferentially satisfied. Moreover, the operational constraints of the VCS are included in Eq. (5). As the constraints for the control input $\boldsymbol{u}_{\mathrm{VCS}}$, the lower and upper limits, $\underline{\boldsymbol{U}}_{\mathrm{VCS}}$ and $\bar{\boldsymbol{U}}_{\mathrm{VCS}}$, respectively, and the ramp rate limit, $\overline{\Delta \boldsymbol{U}}_{\mathrm{VCS}}$, are considered:

$$\left.\begin{aligned} \underline{\boldsymbol{U}}_{\mathrm{VCS}} \le \boldsymbol{u}_{\mathrm{VCS}}(t_j) &\le \bar{\boldsymbol{U}}_{\mathrm{VCS}} \\ \left|\Delta \boldsymbol{u}_{\mathrm{VCS}}(t_j)\right| &\le \overline{\Delta \boldsymbol{U}}_{\mathrm{VCS}} \end{aligned}\right\} \qquad (j = k+1, \cdots, k+N_{\mathrm{C}}) \tag{5}$$

As shown in Eq. (6), the control input at the initial sampling time t_k is provided as a parameter $\boldsymbol{U}_{\mathrm{VCS}}$ because it was transmitted to the lower-level control at the previous sampling time.

$$\boldsymbol{u}_{\mathrm{VCS}}(t_k) = \boldsymbol{U}_{\mathrm{VCS}}(t_k) \tag{6}$$

Equation (7) shows the lower and upper limits for the system output, $\underline{\boldsymbol{Y}}_{\mathrm{VCS}}$ and $\overline{\boldsymbol{Y}}_{\mathrm{VCS}}$, respectively:

$$\underline{\boldsymbol{Y}}_{\mathrm{VCS}} \le \boldsymbol{y}_{\mathrm{VCS}}(t_j) \le \overline{\boldsymbol{Y}}_{\mathrm{VCS}} \qquad (j = k+1, \cdots, k+N_{\mathrm{C}}) \tag{7}$$

Equation (8) is the demand response constraint. The shortfall in the power consumption reduction during the demand response $\varepsilon_{\mathrm{DR}}$ (kWh) is considered so that the optimal control problem may not be infeasible when the demand response request is not satisfied:

$$\left.\begin{aligned} &\sum_{j=j_{\mathrm{DR}}^{\mathrm{STA}}(i)}^{J_{\mathrm{DR}}} \{E_{\mathrm{VCS}}^{\mathrm{BL}}(i) - e_{\mathrm{VCS}}(t_j)\}\Delta T_{\mathrm{U}} + \varepsilon_{\mathrm{DR}}(i) \ge S_{\mathrm{DR}}\Delta T_{\mathrm{DR}} \\ &\varepsilon_{\mathrm{DR}}(i) \ge 0 \end{aligned}\right\} \quad (i = 1,2,\ldots,I) \tag{8}$$

where $E_{\mathrm{VCS}}^{\mathrm{BL}}$ is the parameter expressing the power consumption in the baseline operation (kW); e_{VCS} is the power consumption of the VCS (kW) and included in the system output vector $\boldsymbol{y}_{\mathrm{VCS}}$; S_{DR} is the parameter expressing the power consumption reduction requested during the demand response period; $j_{\mathrm{DR}}^{\mathrm{STA}}$ is the sampling number corresponding to the start of the demand response period; and J_{DR} is the total number of sampling times in the one evaluation slot of the demand response achievement, i.e., $J_{\mathrm{DR}} = \Delta T_{\mathrm{DR}}/\Delta T_{\mathrm{U}}$.

4.2.1.3. Objective function

The objective function to be minimized is the weighted sum of the electricity cost, the shortfall in the power consumption reduction during the demand response period, the variation in the compressor speed, and the margin of the indoor temperature from its upper limit as follows:

$$\begin{aligned} J = &\sum_{j=k}^{k+N_{\mathrm{C}}} \left[\Phi(t_j) e_{\mathrm{VCS}}(t_j)\Delta T_{\mathrm{U}}\right] + W_1 \sum_{i=1}^{I} \varepsilon_{\mathrm{DR}}^{\mathrm{S}}(i) + W_2 \sum_{j=k+1}^{k+N_{\mathrm{C}}-1} \left[n_{\mathrm{CP}}(t_j) - n_{\mathrm{CP}}(t_{j-1})\right]^2 \\ &- W_3 \sum_{j=k_{\mathrm{DR}}^{\mathrm{STA}}+1}^{k_{\mathrm{DR}}^{\mathrm{STA}}+N_{\mathrm{DR}}} \left[\bar{\theta}_{\mathrm{RM}} - \theta_{\mathrm{RM}}(t_j)\right] \end{aligned} \tag{9}$$

where $k_{\mathrm{DR}}^{\mathrm{STA}}$ is the sampling number in the control horizon expressing at the start of the demand response period; Φ is the parameter expressing the time-varying electricity price (JPY/kWh); n_{CP} is the compressor speed (rpm) and included in the control input vector $\boldsymbol{u}_{\mathrm{VCS}}$; N_{DR} is the total number of sampling times of the demand response period, i.e., $N_{\mathrm{DR}} = H_{\mathrm{DR}}/\Delta T$; and W_1, W_2, and W_3 are the parameters expressing the weight coefficients. The third term is included to prevent rapid changes in the compressor speed for VCS stable operation. By considering the fourth term, a margin for the hard constraint of indoor comfort is provided under the actual operation of the VCS with nonlinear performances. The formulated problem results in a quadratic programming problem because the quadratic term is included in the objective function of Eq. (9).

4.3. VCS linearizer

The linear static model of the VCS of Eq. (1) is generated by performing linearization before solving the optimal control problem. The static simulation model of the VCS [10] can be expressed by the following equation:

$$\left.\begin{aligned} &\boldsymbol{y}_{\mathrm{VCS}} = \boldsymbol{f}_{\mathrm{VCS}}(\boldsymbol{u}_{\mathrm{VCS}}, \boldsymbol{x}_{\mathrm{RM}}) \\ &\boldsymbol{y}_{\mathrm{VCS}} = [n_{\mathrm{CP}}, l_{\mathrm{EV}}, Q_{\mathrm{S}}, Q_{\mathrm{L}}, e_{\mathrm{VCS}}]^{\mathrm{T}} \\ &\boldsymbol{u}_{\mathrm{VCS}} = \left[p_{\mathrm{CP}}^{\mathrm{IN}}, \theta_{\mathrm{EP}}^{\mathrm{SH}}, g_{\mathrm{CD}}, g_{\mathrm{EP}}\right]^{\mathrm{T}} \\ &\boldsymbol{x}_{\mathrm{RM}} = [\theta_{\mathrm{RM}}, w_{\mathrm{RM}}, \theta_{\mathrm{A}}]^{\mathrm{T}} \end{aligned}\right\} \tag{10}$$

where $\boldsymbol{f}_{\mathrm{VCS}}$ is the vector expressing the set of static model formula of the VCS [10]; l_{EV} is the expansion valve opening; Q_{S} and Q_{L} are the sensible and latent heat output of the VCS, respectively; $p_{\mathrm{CP}}^{\mathrm{IN}}$ is the compressor inlet pressure; $\theta_{\mathrm{EP}}^{\mathrm{SH}}$is the degree of superheat at the refrigerant at the evaporator outlets; g_{CD} and g_{EP} are the air volumetric flow rate of the condenser and evaporator, respectively; and θ_{A} is the ambient temperature. $\boldsymbol{f}_{\mathrm{VCS}}$ can be effectively solved by our decomposition-based solution method [10].

The coefficient matrices $\boldsymbol{A}_{\mathrm{U}}(t)$ and $\boldsymbol{A}_{\mathrm{X}}(t)$ of the linear static model of the VCS can be generated by linearizing with Eq. (10) at the current operating points, i.e., $\boldsymbol{u}_{\mathrm{VCS}}(t)$ and $\boldsymbol{x}_{\mathrm{RM}}(t)$, as follows:

$$\boldsymbol{A}_{\mathrm{U}}(t) = \left[\frac{\partial \boldsymbol{f}_{\mathrm{VCS}}\left(\boldsymbol{u}_{\mathrm{VCS}}(t), \boldsymbol{x}_{\mathrm{RM}}(t)\right)}{\partial p_{\mathrm{CP}}^{\mathrm{IN}}(t)}, \frac{\partial \boldsymbol{f}_{\mathrm{VCS}}\left(\boldsymbol{u}_{\mathrm{VCS}}(t), \boldsymbol{x}_{\mathrm{RM}}(t)\right)}{\partial \theta_{\mathrm{EVA}}^{\mathrm{SH}}(t)}, \frac{\partial \boldsymbol{f}_{\mathrm{VCS}}\left(\boldsymbol{u}_{\mathrm{VCS}}(t), \boldsymbol{x}_{\mathrm{RM}}(t)\right)}{\partial g_{\mathrm{CD}}^{\mathrm{A}}(t)}, \frac{\partial \boldsymbol{f}_{\mathrm{VCS}}\left(\boldsymbol{u}_{\mathrm{VCS}}(t), \boldsymbol{x}_{\mathrm{RM}}(t)\right)}{\partial g_{\mathrm{EP}}^{\mathrm{A}}(t)}\right] \quad (11)$$

$$\boldsymbol{A}_{\mathrm{X}}(t) = \left[\frac{\partial \boldsymbol{f}_{\mathrm{VCS}}\left(\boldsymbol{u}_{\mathrm{VCS}}(t), \boldsymbol{x}_{\mathrm{RM}}(t)\right)}{\partial \theta_{\mathrm{RM}}(t)}, \frac{\partial \boldsymbol{f}_{\mathrm{VCS}}\left(\boldsymbol{u}_{\mathrm{VCS}}(t), \boldsymbol{x}_{\mathrm{RM}}(t)\right)}{\partial x_{\mathrm{RM}}(t)}, \frac{\partial \boldsymbol{f}_{\mathrm{VCS}}\left(\boldsymbol{u}_{\mathrm{VCS}}(t), \boldsymbol{x}_{\mathrm{RM}}(t)\right)}{\partial \theta_{\mathrm{A}}(t)}\right] \quad (12)$$

The linearization in Eqs. (11) and (12) is performed using the central difference. $\boldsymbol{A}_0$ is calculated as follows:

$$\boldsymbol{A}_0(t) = \boldsymbol{f}_{\mathrm{VCS}}(\boldsymbol{u}_{\mathrm{VCS}}(t), \boldsymbol{x}_{\mathrm{RM}}(t)\ ) - \boldsymbol{A}_{\mathrm{U}}(t)\boldsymbol{u}_{\mathrm{VCS}}(t) - \boldsymbol{A}_{\mathrm{X}}(t)\boldsymbol{x}_{\mathrm{RM}}(t) \quad (13)$$

4.3. PMV calculator

The PMV is calculated as the measure of indoor comfort from the air temperature, air humidity, wind speed, radiative temperature, metabolic equivalent, and amount of clothing [11]. In the PMV calculator, wind speed, metabolic equivalent, and amount of clothing are provided as the parameters. The radiative temperature is assumed to be equal to the air temperature, as is the case with the previous studies [12]. Consequently, the PMV is calculated from the air temperature and absolute humidity measured at the current sampling time.

5. Potential evaluation of demand response by VCS

5.1. Calculation conditions

The developed demand response framework using model predictive control is applied to the coupled system of a VCS and an air-conditioned room. The calculation conditions, including the system specifications, the simulation conditions, the control conditions, and the cooling load condition, are summarized in this subsection.

5.1.1. Specifications of VCS and air-conditioned room

The target VCS consists of one outdoor unit and two indoor units. The condenser in the outdoor unit is a plate-fin and tube-type heat exchanger and the evaporators in the indoor units are cross-fin tube-type heat exchangers. The working refrigerant is R410A. The specifications of the VCS components are listed in Table 1. The refrigerant charge amount is set at 6 kg.

The specifications of the target air-conditioned room are listed in Table 2. A southeast-facing office building in Japan is assumed.

Table 1: Specifications of VCS components.

System component	Item		Value
Condenser	Heat transfer area (refrigerant / air side)	m^2	3.86 / 85.8
	Inside diameter of tube	m	6.73×10^{-3}
	Outside diameter of tube	m	7.37×10^{-3}
	Number of tubes		112
Evaporator	Heat transfer area (refrigerant / air side)	m^2	2.73 / 41.53
	Inside diameter of tube	m	6.73×10^{-3}
	Outside diameter of tube	m	7.37×10^{-3}
	Number of tubes		168
Compressor	Discharge displacement	m^3	6.58×10^{-5}

Table 2: Specifications of air-conditioned room.

Item		Value
Floor area	m^2	170.0
Floor height	m	2.7
Sensible heat capacity	kJ/K	7105
Latent heat capacity	kJ/(kg/kg)	1.836×10^{6}

5.1.2. SImulation conditions

In the static simulation of the VCS [10], the performance characteristics of the heat exchangers, i.e., the condenser and evaporators, are formulated using a distributed parameter model. The properties of R410A were previously calculated using REFPROP Ver. 10.0, and their look-up tables were generated.

5.1.3. Control conditions

In accordance with the capacity market scheme in Japan, the demand response is requested three hours before. The demand response period, i.e., $H_{\mathrm{DR}} = I\Delta T_{\mathrm{DR}}$, is set at three hours, i.e., 15:00–18:00. The interval for the evaluation slot ΔT_{DR} is set at 30 minutes. The requested reduction in the power consumption S_{DR} varies in the range from 0.3 kW to 0.8 kW. If the demand response request is noticed, the control horizon involves the demand response period, and the horizon length is shortened with the sampling time evolution. The power consumption in the baseline operation is the result of the model predictive control without the demand response under the same calculation conditions.

The control interval of the model predictive control ΔT_{U} was set at 5 min, and the default number of sampling times in the control horizon N is 36 because the default control horizon length is three hours. The electricity price Φ is fixed at 21.12 [JPY/kWh]. The operational constraints of the VCS in the model predictive control are listed in Table 3; the continuous operation of the VCS is focused on. The metabolic equivalent and amount of clothing to calculate the PMV were based on the literature [13]. The weight coefficients in Eq. (9) were determined through a trial-and-error process. The optimal control problem was coded in PICOS Ver. 2.4.17, which is a Python API, and solved by using Gurobi Ver. 12.0.1. The model predictive controller coded in PICOS and our static simulation coded in C++ are coupled in a Python environment.

5.1.4. Cooling load conditions

The sensible and latent cooling loads according to variations in solar radiation, ambient temperature, and occupancy states are simulated using a whole-building energy simulation program, EnergyPlus [14]. The potential of the demand response by the VCS is evaluated on eight candidate days for activating the demand response in Osaka, Japan, i.e., July 25, July 26, August 2, August 4, August 30, September 11, September 13, and September 15 in 2022. These candidate days satisfy the following conditions: 1) high ambient temperature from the afternoon to the night, 2) short duration of solar radiation in the afternoon, and 3) the total power demand in this area close to its forecasted value. The measured ambient temperature, duration of solar radiation, and the simulated cooling load are shown in Fig. 5.

It is assumed that the predictor in the model predictive control can perfectly predict the variations in the cooling loads. The initial values of the indoor temperature and absolute humidity were set at 298.71 K and 0.00877 kg/kg, respectively, so that the PMV value is 0.0.

Table 3: Operational constraints of VCS in model predictive control.

Variables	Lower limit	Upper limit	Ramp rate limit
Compressor speed	1200 rpm	6000 rpm	15 rpm/s
Expansion valve opening	0 %	100 %	25 %/s
Outdoor airflow rate	80 %	100 %	10 %/s
Indoor airflow rate	80 %	100 %	10 %/s
Compressor inlet pressure	0.895 MPa	1.40 MPa	
Degree of superheat at evaporator outlet	3.0 K	3.0 K	
PMV (Predicted Mean Vote)	-0.5	0.5	

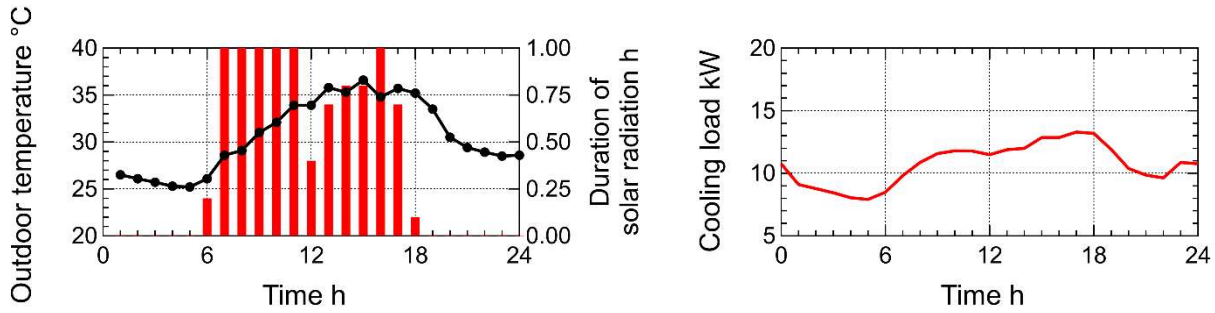

(a) Outdoor temperature and solar radiation duration (b) Cooling load

Figure 5: Outdoor and cooling load conditions on July 26.

5.2. Potential evaluation of demand response

The control planning result of the VCS and air-conditioned room to the demand response activation with the requested reduction in the power consumption S_{DR} of 0.5 kW on July 26 is shown in Fig. 6; the indoor temperature and absolute humidity, the power consumption, the cooling capacity, the compressor inlet pressure, and the compressor speed are focused on. The colored band in Fig. 6(a) is the comfort zone of the indoor temperature satisfying the PMV constraint. The gray-colored area indicates the demand response period, i.e., 15:00–18:00. The control planning result of the baseline operation is also presented.

In the baseline operation, the indoor temperature is maintained at values close to the upper limit of the comfort zone. The cooling capacity tracks the variations in the cooling load colored in green. This is a typical behavior of the model predictive control to minimize the electricity cost under the satisfaction of the indoor comfort constraint [1]. The noteworthy behavior in the demand response is the pre-cooling of the air-conditioned room before the demand response period. After receiving the demand response request at 12:00, the cooling capacity is greatly increased so that the indoor temperature at the start of the demand response period is close to its lower limit satisfying indoor comfort. The power consumption and cooling capacity during the demand response period are lower than those in the baseline operation so as to satisfy the demand response constraint of Eq. (8). By virtue of the pre-cooling planning, the indoor temperature continuously increases during the demand response period and reaches its upper limit at the terminal of the demand response period. To satisfy the demand response constraint at every 30 minute-time slot, the power consumption, cooling capacity, compressor inlet pressure, and compressor speed fluctuate in 30 minutes period.

The control planning results in the demand response activation with the requested reduction in the power consumption S_{DR} of 0.8 and 0.3 kW on July 26 are shown in Figs. 7 and 8, respectively. In any S_{DR}, the pre-

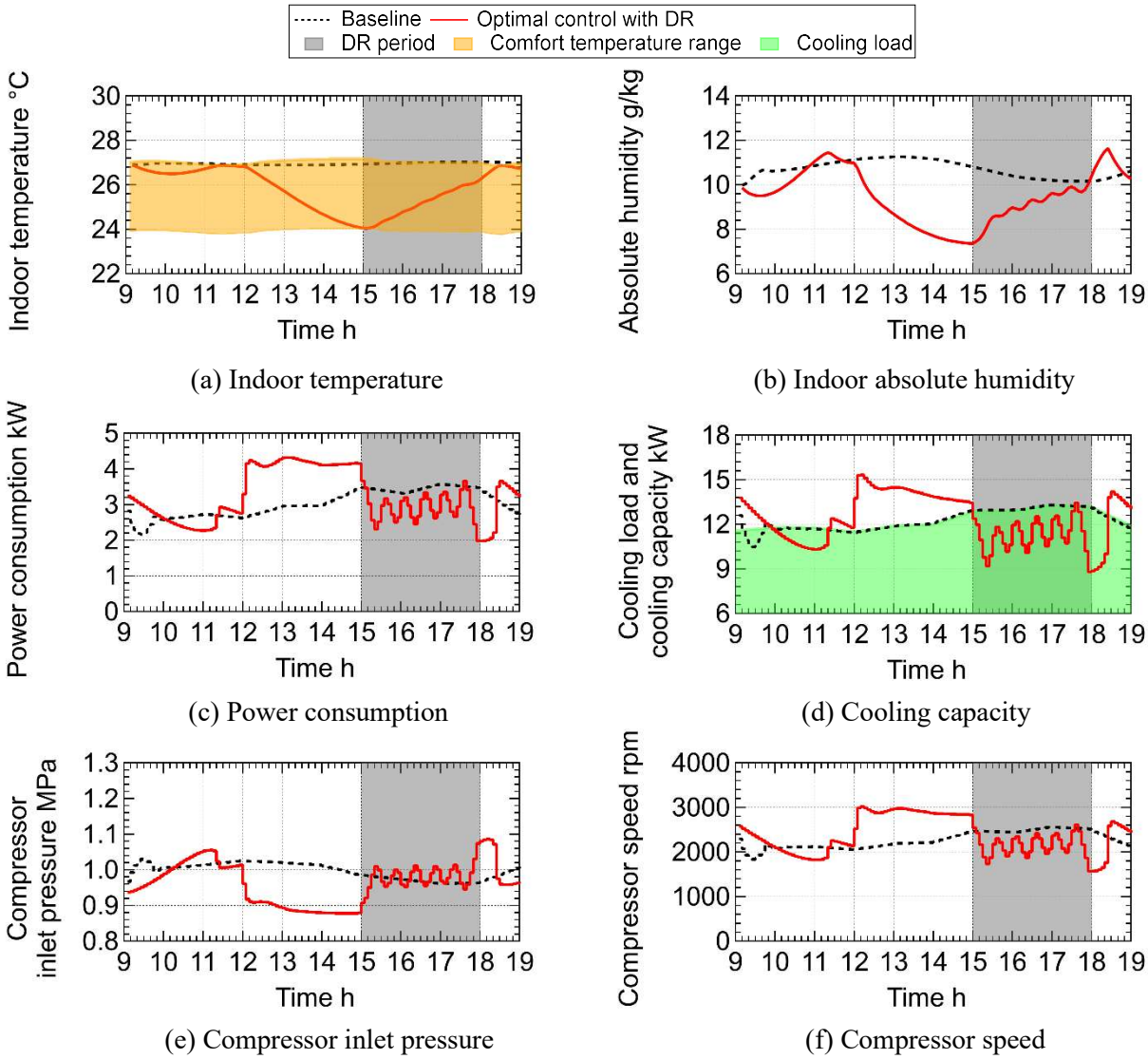

Figure 6: Optimal control planning result of VCS and air-conditioned room on July 26. (Requested reduction in power consumption: 0.5 kW)

cooling behavior is the same, and the indoor temperature is varied within the comfort zone based on the PMV constraint. However, in S_{DR} = 0.8 kW, the power consumption of the VCS during the demand response period fluctuates widely and sometimes surpasses that in the baseline operation. This means that the pre-cooling under the rated compressor inlet pressure is insufficient to reduce more power consumption in the demand response period. In S_{DR} = 0.3 kW, the power consumption of the VCS is also more than that in the baseline at the final time slot of the demand response period. This is due to a large margin of the indoor temperature to the upper limit of the comfort zone, which is caused by the same weight coefficients in Eq. (9) in any S_{DR}.

Table 4 lists the achievement of the demand response request at each time slot evaluated in six cases of the requested reduction in the power consumption S_{DR}. In S_{DR} = 0.4, 0.5, 0.6, and 0.7 kW, the demand response request can be achieved at all the 30-minute time slots. In S_{DR} = 0.3 and 0.8 kW, the demand response request is not satisfied at the final time slot and several time slots, respectively. This result indicates that there is an upper limit as well as a lower limit of the demand response potential, i.e., the requested reduction in the power consumption S_{DR}.

Finally, the total achievement of the demand response request in S_{DR} = 0.3, 0.5, and 0.8 kW on the eight candidate days for activating the demand response is listed in Table 5. In S_{DR} = 0.5 kW, the demand response request is perfectly achieved on the eight candidate days. However, in S_{DR} = 0.8 kW, the demand response request is not achieved on any candidate day because the requested reduction in the power consumption is too large for this VCS. In S_{DR} = 0.3 kW, the demand response request is violated on hot candidate days. i.e., July 25, July 26, August 2, and August 4, on which the ambient temperature during the demand response period is close to or higher than 35 °C.

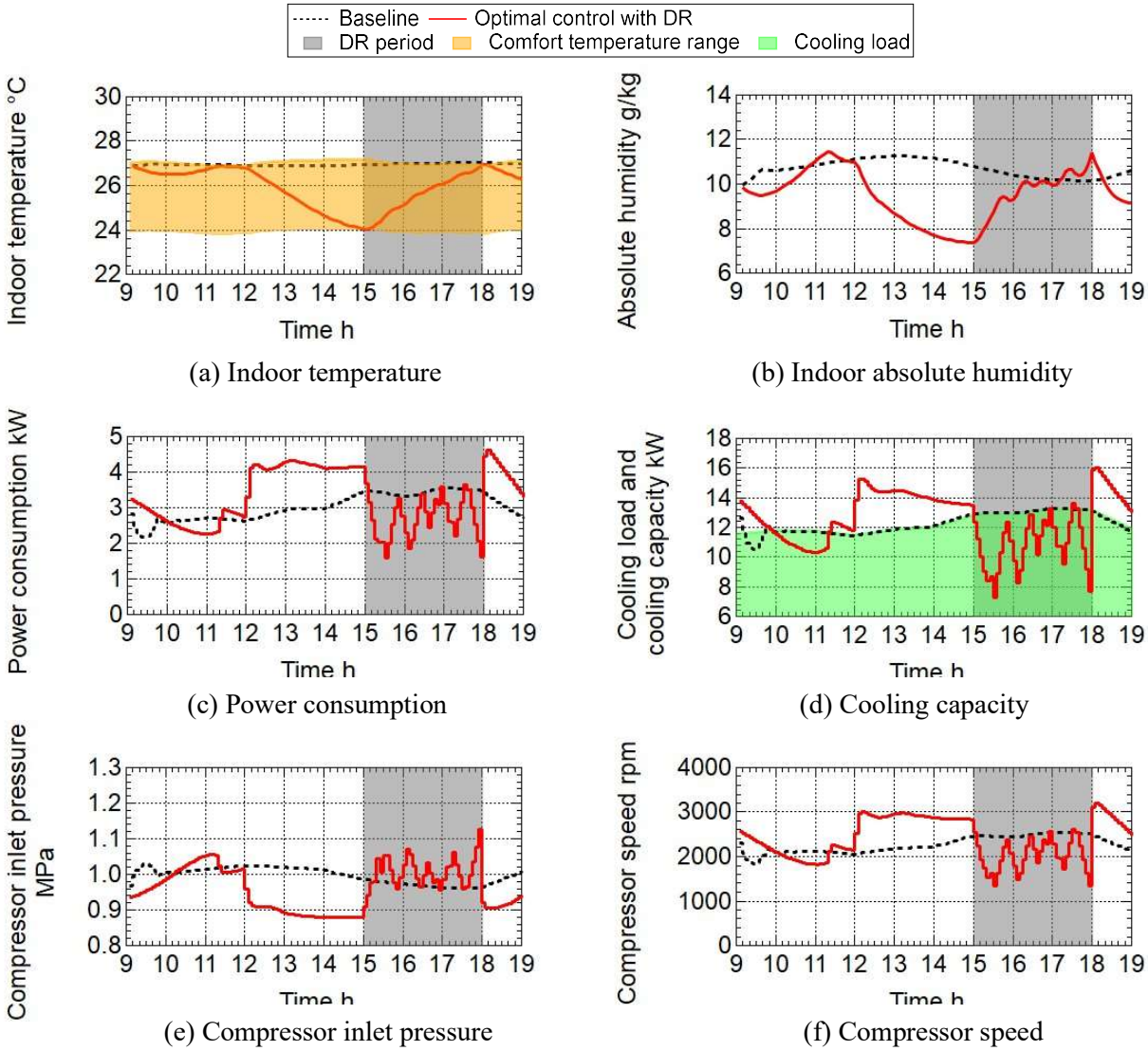

(a) Indoor temperature (b) Indoor absolute humidity

(c) Power consumption (d) Cooling capacity

(e) Compressor inlet pressure (f) Compressor speed

Figure 7: Optimal control planning result of VCS and air-conditioned room on July 26.
(Requested reduction in power consumption: 0.8 kW)

Table 4: Demand response achievement evaluation on July 26.

Time slot	Requested reduction in power consumption kW					
	0.3	0.4	0.5	0.6	0.7	0.8
15:00–15:30	✓	✓	✓	✓	✓	✓
15:30–16:00	✓	✓	✓	✓	✓	✓
16:00–16:30	✓	✓	✓	✓	✓	✓
16:30–17:00	✓	✓	✓	✓	✓	
17:00–17:30	✓	✓	✓	✓	✓	✓
17:30–18:00		✓	✓	✓	✓	

✓: Achievement of demand response request

6. Conclusions

A model predictive control-based demand response framework for individual VCSs was developed, and the demand response potential was evaluated in a commercial office building application. The demand response framework is composed of a model predictive controller, a VCS linearizer, and a PMV calculator. In the model predictive controller, the optimal control problem, minimizing the weighted sum of the electricity cost, the shortfall in the power consumption reduction during the demand response period, the variation in the compressor speed, and the margin of the indoor temperature from its upper limit, is sequentially solved using a receding horizon approach. To address VCS nonlinearity, a linear model is regenerated in response to changes in the VCS operating point and in indoor and ambient temperatures; this model is then given to the model predictive controller. The control horizon length varies based on demand response requests.

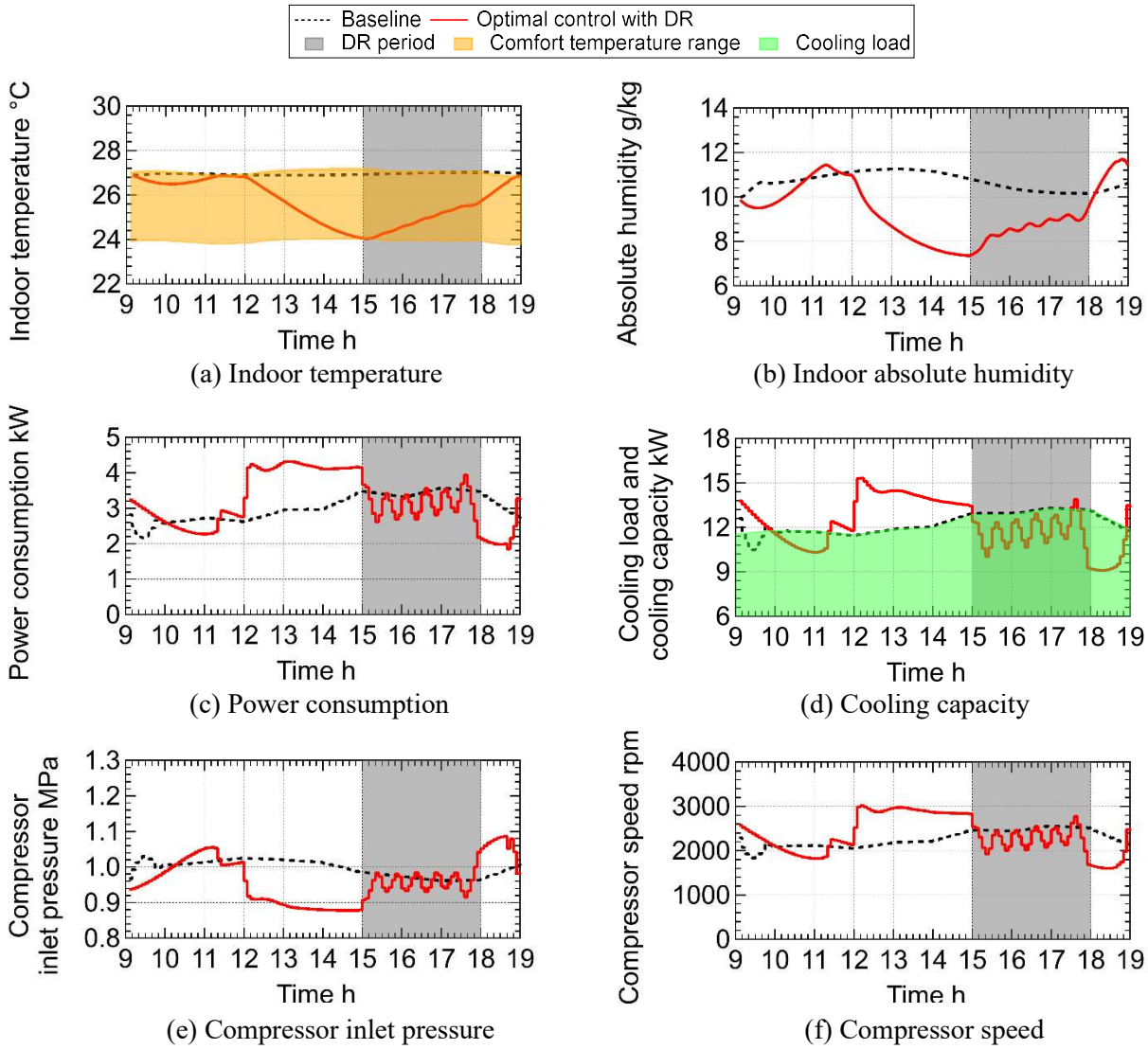

(a) Indoor temperature (b) Indoor absolute humidity

(c) Power consumption (d) Cooling capacity

(e) Compressor inlet pressure (f) Compressor speed

Figure 8: Optimal control planning result of VCS and air-conditioned room on July 26. (Requested reduction in power consumption: 0.3 kW)

Table 5: Demand response achievement evaluation on eight candidate days.

Candidate day	Requested reduction in power consumption kW		
	0.3	0.5	0.8
7/25		✓	
7/26		✓	
8/2		✓	
8/4		✓	
8/30		✓	
9/11	✓	✓	
9/13	✓	✓	
9/15	✓	✓	

✓: Achievement of demand response request in all the time slots

The developed framework is applied to the potential assessment of the demand response by a VCS in an office building. The demand response potential (achievement) is evaluated by varying the requested reduction in the power consumption on eight candidate days for activating the demand response. The results show that the achievement of the demand response request depends on the requested reduction in the power consumption and the VCS pre-cooling capability, which are greatly affected by the ambient temperature. An upper limit as well as a lower limit of the demand response potential were also observed.

In future works, the prediction of the cooling load and the power consumption in the baseline operation should be combined with this demand response framework. A demonstration in the summer season for these purposes will also be performed. A robust controller for the uncertainty of the prediction and many system parameters, including VCS performances, heat insulation properties of air-conditioned rooms, and weight coefficients in the objective function, should be developed.

References

[1] Wakui T., Matsumoto T., Yokoyama, R., Proceedings of the 35th International Conference on Efficiency, Cost, Optimization, Simulation and Environmental Impact of Energy Systems (ECOS 2022), pp. 2127–2138.

[2] Yamazaki T., Takano H., Asano H., Journal of Japan Society of Energy and Resources 2022; 43 (6): 266–273.

[3] Dullinger C., Struckl W., Kozek M., Applied Thermal Engineering 2018; 128: 1646–1659.

[4] Elliott M.S., Rasmussen B.P., Control Engineering Practice 2013; 21 (12): 1665–1677.

[5] Wang C., Wang B., Cui M., and Wei F., Energy and Buildings 2022; 256: Paper No. 111708, p. 1–12.

[6] Tang L., Xie H., Wang Y., and Xu Z., Applied Energy 2025; 388: Paper No. 125631.

[7] Wang C., Wang B., and You F., Applied Energy 2024; 369: Paper No. 123581

[8] Organization for Cross-Regional Coordination of Transmission Operators (OCCTO), 2021 – Available at:<https://www.occto.or.jp/en/about_occto/securing.html>[accessed 17.4.2026]

[9] Yan H., Deng S., Chan M., Applied Thermal Engineering 2016; 100: 880–892.

[10] Wakui T., Okamura H., Yokoyama R., Proceedings of the 33rd International Conference on Efficiency, Cost, Optimization, Simulation and Environmental Impact of Energy Systems (ECOS 2020), pp. 1005–1017.

[11] ISO 7730:2005

[12] Farzaneh Y., Tootoonchi A.A., Applied Thermal Engineering 2008; 28 (14-15): 1906–1917.

[13] Azizpour F., Moghimi S., Lim C.H., Mat S., Salleh E., Sopian K., Indoor and Built Environment 2013; 22 (5): 836–845.

[14] National Renewable Energy Laboratory (NREL) (2017). EnergyPlus™.

Acknowledgments

This study was conducted on the basis of the collaborative project with Daigas Energy Co., Ltd. in 2024 and 2025 and JSPS KAKENHI Grant Number JP24K08326.